Fluid Dynamics and Diffusion Calculations for Laminar Liquid Jets

L. E. SCRIVEN and R. L. PIGFORD

University of Delaware, Newark, Delaware

In connection with a study of the mechanism of gas absorption the problem arose of predicting absorption rates into laminar liquid jets. A solution to the problem is presented in this paper, which provides an example of the application of fluid dynamics to the analysis of mass transfer in a complex flow system.

The water jets considered here issued from circular nozzles of about 1.5-mm diameter, flowed intact downward through an atmosphere of solute gas at average velocities of from 75 to 550 cm./sec. over distances of 1 to 15 cm., and were collected in a receiver slightly larger in diameter than the nozzles. Equations describing the liquid flow near the jet surface are deduced from measurements of jet diameter and analogy to related flow situations. When one uses these equations, absorption rates are predicted from unsteady state diffusion theory with the assumption of interfacial equilibrium. The predicted rates for carbon dioxide at 25°C are in close agreement with experimental determinations over the observed range of contact time of the liquid with gas, namely 0.003 to 0.04 sec.

Laminar liquid jets possess several attractive advantages over other types of apparatus for fundamental studies of the mechanism of gas absorption. To obtain a valid experimental test of unsteady state diffusion theory in a flow system, it is imperative that the fluid dynamics of the system be known accurately. The area of contact between gas and liquid must be known, and furthermore the nominal time of exposure of liquid to gas should be of the order of 0.001 to 1 sec., since exposure times of these magnitudes are encountered in most contacting equipment of practical interest. If there is departure from equilibrium at the interface, the effect of an interfacial resistance on absorption rates is likely to be greater the shorter the period of exposure of liquid to gas, simply because the shorter the contact time the smaller the bulk-phase diffusional resistance to mass transfer.

Bubbles of gas rising through liquid are manifestly unsuitable, for the flow regime in the vicinity of the bubble surface is not well understood (*1*) and probably is strongly influenced by the presence of traces of surface-active contaminants (*9*). Falling droplets of liquid likewise suffer the considerable shortcoming of poorly understood fluid dynamics (*10*). A well-behaved moving film of liquid satisfies the requirements, except that end effects at the points at which the film is brought into and out of contact with the gas seem unavoidable, although they may be minimized to a certain extent through apparatus design and experimental technique. Unfortunately the fluid dynamics of the oft-employed wetted-wall column is usually complicated by rippling, which may be either the cause or an indication of mixing within the falling liquid film (*19*). Rippling can be greatly decreased by the addition of small amounts of surface-active agents to the liquid feed or altogether eliminated by reducing the length of the column sufficiently. However the first practice raises new uncertainties on account of possible interaction between solute and surfactant, while the second promotes the end effects to major importance (*11*). Recently the idea of carrying a liquid film on a moving solid surface has been put to use by Danckwerts and Kennedy (*3*) in their novel rotating-drum apparatus, which appears to be nearly free of appreciable end effects for most operating conditions.

Laminar liquid jets, which have been utilized in surface tension studies for many years (*14*), are well suited for absorption measurements. By employing long, fast-moving jets the end effects at the nozzle and the collection device can be reduced to insignificance, but the influences of viscous drag in the nozzle and gravitational acceleration on flow and absorption must be assessed, as they are herein. Previous investigators (*4, 5, 13, 18*) have overlooked these complications, with the exception of Cullen and Davidson (*2*), who discussed qualitatively the influence of gravity insofar as it affects the axial velocity distribution and who evidently succeeded by judicious nozzle design in greatly reducing the influence of viscosity. Contact area can be evaluated readily from measurements of jet diameter. A particular advantage of jets is the wide range of liquid contact times which can be achieved with them, down to a few milli-seconds or even less.

APPARATUS

Detailed descriptions have been given elsewhere of the gas-absorption apparatus in which the jets of interest here were produced (*16, 17*). In brief, a jet of water issued from a circular nozzle about 1.5-mm. I.D. flowed intact downward at an average velocity of from 75 to 550 cm./sec. over a distance of 1 to 15 cm. and was collected in a glass capillary receiver about 2 mm. I.D. The receiver and a nozzle are shown in Figure 1. Between the nozzle and receiver the surface of the jet was exposed to an atmosphere of solute gas confined within a glass chamber. The apparatus was similar to that used by Matsuyama (*13*), Manogue (*12*), and Eipper (*6*).

It was possible to collect the entire jet in the receiver for prolonged periods of operation without entraining any gas bubbles in the liquid, provided the nozzle and receiver were accurately aligned, the resistance to flow downstream of the receiver was carefully adjusted, and strong vibrations were eliminated. Operating

L. E. Scriven is with the Shell Development Company, Emeryville, California.

troubles, when they occurred, seemed to arise from occasional small fluctuations in the liquid feed rate.

FLUID DYNAMICS

Diameter Measurements

As the first step in analyzing the fluid dynamics of the jet, measurements were made with a Gaertner traveling microscope of the jet diameter vs. length across three diameters 60 deg. apart. Measurements made at two flow rates have been plotted in Figure 2.

From these was inferred the velocity distribution. It was assumed that the velocity within the core of the jet issuing from the nozzle was uniform and that outside the core there existed an annular boundary layer in which the velocity was reduced, in consequence of the frictional drag exerted by the inside surface of the nozzle. It was supposed that after the jet left the nozzle, momentum interchange between the core and boundary layer would have produced a substantially flat velocity profile beyond some not-too-distant downstream point. By assuming that the velocity distribution within the boundary layer at the nozzle could be adequately represented by a cubic equation, one gets

$$\frac{U}{U_\infty} = \frac{3}{2}\left(\frac{Y}{\delta}\right) - \frac{1}{2}\left(\frac{Y}{\delta}\right)^3, \qquad 0 \le Y \le \delta \tag{1}$$

$$\frac{U}{U_\infty} = 1, \qquad \delta \le Y \le R_0 \tag{2}$$

and writing mass and momentum balances between the face of the nozzle and a downstream point corresponding to a flat velocity profile (Figure 3), one obtains the following approximate expression relating boundary-layer thickness to the measured diameters:

$$b \equiv \frac{\delta}{R_0} = 2.094\left[\left(\frac{R_0}{R}\right)^2 - 1 - \frac{\pi^2 g_L R_0^4 X}{4q^2}\left(\frac{R_0 + R}{R_0}\right)^2\right] \tag{3}$$

The length of flat plate oriented parallel to the direction of flow which would be required to produce a boundary layer of thickness, if one assumes a cubic velocity distribution, is given by (*15*):

$$l = \left(\frac{13}{280}\right)\frac{U_\infty}{\nu}\,\delta^2 \tag{4}$$

Values of b and l calculated from the data presented in Figure 2 are given in Table 1; it is apparent from the near constancy of b that the velocity profiles within the jets were indeed very nearly flat after 5 cm. or less of travel. This conclusion is borne out by a further est of the data. Downstream from the nozzle in a vertical jet the velocity profile becomes nearly flat, the principal force acting is gravity, and the variation of velocity with jet length is given to a close approximation by [see the discussion of Equation (9)]

$$U = \sqrt{U_0^2 + 2g_L X} \tag{5}$$

Table 1

Flow, q, cc./sec.	Distance, X, cm.	Diameter, D, cm.	$b \equiv \delta/R_0$	Average length, l, cm.
5.02	0	0.1543		
	5	0.1454	0.103	
	10	0.1419	0.098	0.088
	15	0.1385	0.098	
2.58	0	0.1546		
	3	0.1406	0.114	
	5	0.1362	0.095	0.043
	7	0.1320	0.099	

From this expression and the equation of continuity it follows that

$$\frac{D}{D_0} = \left(1 + \frac{\pi^2 g_L D_0^4 X}{8q^2}\right)^{-\frac{1}{4}} \tag{6}$$

The agreement of observed variations of diameter with the behavior predicted by Equation (6) is quite good at downstream distances beyond 2.5 cm. (broken curves in Figure 2).

In passing it should be pointed out that the calculated values of boundary-layer thickness do provide confirmation of the laminar character of the flow in the emerging jet. The Reynolds number based on boundary-layer thickness $U_\infty\delta/\nu$ varies from 100 to 250 for the jets. In contrast the analogous critical Reynolds number for flow over a flat plate is in the range 1,500 to 7,000 (*15*); furthermore the stability of laminar flow is increased in the presence of a favorable pressure gradient as obtained with the nozzle design employed in the present work.

Surface Velocity

To predict absorption rates it is necessary to know the velocity distribution in the liquid at and close to the surface of the jet. For the relatively short contact times of interest in connection with the present study, the penetration depth of the diffusing molecules is very small compared with the jet diameter; therefore detailed knowledge of the flow within the interior of the jet is not required.

Since the boundary-layer thickness at the nozzle, as calculated above, amounted to only one tenth of the nozzle radius, it seemed reasonable to assume that (*a*) the core velocity remained unchanged by momentum exchange with the boundary layer and (*b*) the annular boundary layer could be treated as two dimensional. In addition it was assumed that (*c*) the drag of the surrounding gas on the surface of the jet was negligible, (*d*) the minor complication arising from the small rate of change of diameter with length was also negligible, and (*e*) gravitational acceleration was absent. Except in the region close to the nozzle, where gravitational forces were small compared with viscous shear, the last assumption is a gross oversimplification, as is shown below. But with it the problem of analyzing the velocity distribution in the neighborhood of the jet surface became identical with the problem of calculating the velocity distribution in a laminar wake behind an infinitely thin, flat plate oriented parallel to the direction of flow, as depicted in Figure 3, a problem solved many years ago by Goldstein (*7, 8*). The analogy between the laminar jet and Goldstein's problem was pointed out by Rideal and Sutherland (*14*).

For velocities close to the trailing edge of the flat plate Goldstein used three terms of a series solution obtained by continuation of the classical Blasius solution for a flat plate; for velocities far downstream he obtained first and second approximations to an asymptotic solution:

$$\frac{U_s}{U_\infty} = 1.2262\xi(1 - 0.9631\xi^3 + 2.2068\xi^6) = a_1\xi(1 - a_2\xi^3 + a_3\xi^6), \qquad \xi \equiv \left(\frac{X}{4l}\right)^{\frac{1}{3}}; \quad \frac{X}{4l} \le 0.0486 \tag{7}$$

$$\frac{U_s}{U_\infty} = 1 - \frac{0.1873}{\sqrt{x}} - \frac{0.0176}{x} = 1 - \frac{a_4}{\sqrt{x}} - \frac{a_5}{x}, \qquad x \equiv \frac{X}{4l} + 0.13; \quad \frac{X}{4l} \ge 0.125 \tag{8}$$

Figure 4 reproduces Goldstein's complete curve for surface velocity (velocity downstream in the plane of the flat plate).

At distances downstream of the nozzle of more than about 2.5 cm. the velocity profiles within the jets were very nearly flat, and the flow, insofar as it affected jet diameter, could be approximated by the free-fall Equation (5). In the downstream portions of the jets, then, gravitational effects were far from negligible as assumed in (*e*) above, and in fact they predominated in these regions. Thus another estimate of the liquid velocity in the neighborhood of the jet surface is given by

$$\frac{U_s}{U_0} = \sqrt{1 + \frac{2g_L X}{U_0^2}} \tag{9}$$

Precisely speaking, Equation (9) assumes a strictly one-dimensional flow, although the very slight taper of the

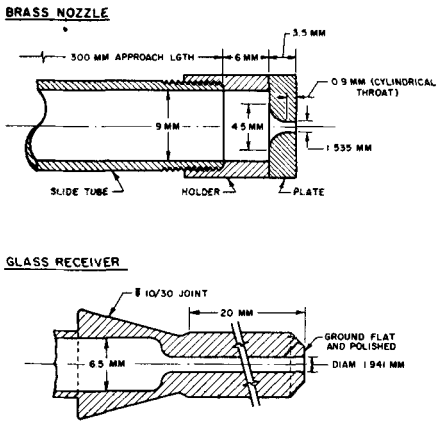

Fig. 1 Jet nozzle and receiver.

jets showed that the flow was in fact two dimensional. Because of the small influence of viscosity and the very nearly uniform jet cross section, however, the assumption of strictly one-dimensional flow neglecting $\partial U/\partial Y$ is felt to yield a very good approximation for U_s far downstream of the nozzle.

From the surface velocity one can easily obtain the component of velocity normal to the surface at small depths beneath the liquid surface. Continuity of an incompressible liquid in two-dimensional flow requires that

$$\frac{\partial U}{\partial X} + \frac{\partial V}{\partial Y} = 0 \qquad (10)$$

But

$$dV = \frac{\partial V}{\partial X}\,dX + \frac{\partial V}{\partial Y}\,dY \qquad (11)$$

$$= \frac{\partial V}{\partial X}\,dX - \frac{\partial U}{\partial X}\,dY \qquad (12)$$

$$\int_{X,0}^{X,Y} dV = -\int_0^Y \frac{\partial U}{\partial X}\,dY = -\frac{d}{dX}\int_0^Y U\,dY \qquad (13)$$

Also $V(X, 0) = 0$, and furthermore $U \cong U_s$ is nearly independent of Y in the vicinity of the surface; hence

$$V \cong -Y\frac{dU_s}{dX} \qquad (14)$$

ABSORPTION

Diffusion Equation

The absorption of a slightly soluble, nonreacting gas is governed by the equation for ordinary diffusion in a binary system, with constant diffusivity and mass density:

$$\frac{\partial C}{\partial t} + (\mathbf{v}\cdot\nabla)C = \mathfrak{D}\nabla^2 C \qquad (15)$$

In the jets the penetration depth of the absorbed molecules was much smaller than the jet diameter; consequently the absorbing liquid can be regarded as semi-infinite and its surface as planar. Except in a very small region near the jet surface at the nozzle, diffusion in the axial direction was negligible in comparison with convective transport. Absorption measurements with the jets were made during steady state operation. Under all these conditions Equation (15) simplifies to

$$U\frac{\partial C}{\partial X} + V\frac{\partial C}{\partial Y} = \mathfrak{D}\frac{\partial^2 C}{\partial Y^2} \qquad (16)$$

Furthermore $\partial U/\partial Y$ was very nearly zero at the jet surface (the adjoining gas exerted negligible drag upon the liquid surface) and beneath to a large depth as compared with the penetration depth (*16*); hence U can be replaced by the surface velocity and V can be expressed in terms of U_s by means of Equation (14):

$$U_s\frac{\partial C}{\partial X} - Y\frac{dU_s}{dX}\frac{\partial C}{\partial Y} = \mathfrak{D}\frac{\partial^2 C}{\partial Y^2} \qquad (17)$$

Two boundary conditions appropriate to the problem are

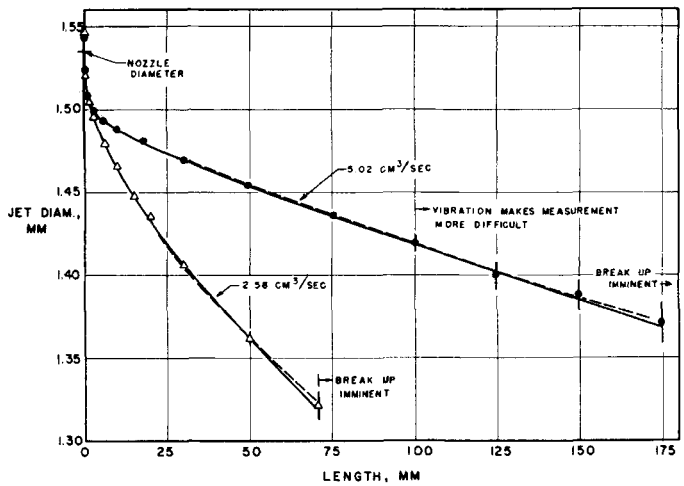

Fig. 2. Jet diameter for 1.535-mm. I. D. paraffin-coated nozzle.

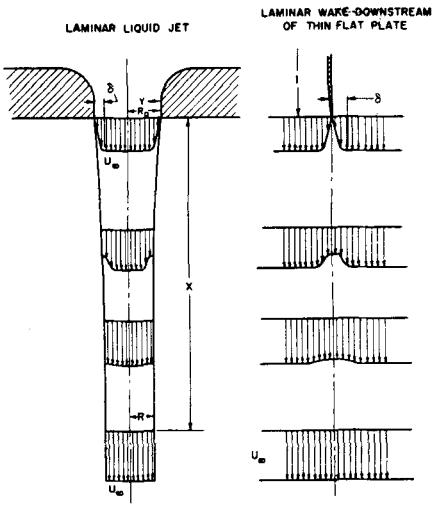

Fig. 3. Velocity Distributions.

$$C(0, Y) = C(X, \infty) = C_0 \qquad (18a, b)$$

If interfacial equilibrium is assumed and heat effects at the interface and gas-phase diffusional resistance are negligible, the third boundary condition is

$$C(X, 0) = C_e \qquad (19)$$

To find a solution of this boundary value problem, one tries the transformation $C(X, Y) = C(\eta)$, where

$$\eta = Yf(X) \qquad (20)$$

Equation (17) then becomes

$$\left(\frac{U_s}{f^3}\frac{df}{dX} - \frac{1}{f^2}\frac{dU_s}{dX}\right)\eta\frac{dC}{d\eta} = \mathfrak{D}\frac{d^2C}{d\eta^2} \qquad (21)$$

If $f(X)$ satisfies

$$\frac{U_s}{f^3}\frac{df}{dX} - \frac{1}{f^2}\frac{dU_s}{dX} = -2\mathfrak{D} \qquad (22)$$

then Equation (21) simplifies to

$$-2\eta\frac{dC}{d\eta} = \frac{d^2C}{d\eta^2} \qquad (23)$$

which, integrated once, gives

$$\frac{dC}{d\eta} = Ae^{-\eta^2} \qquad (24)$$

A second integration, with Equation (18), yields

$$C = C_0 + A\int_\infty^\eta e^{-z^2}\,dz \qquad (25)$$

The remaining constant of integration is evaluated by means of Equation (19); thus

$$\frac{C - C_0}{C_e - C_0} = \frac{2}{\sqrt{\pi}}\int_\eta^\infty e^{-z^2}\,dz \qquad (26)$$

$$= \operatorname{erfc}(\eta)$$

This is the desired solution provided that $f(X)$ satisfies Equation (22), a

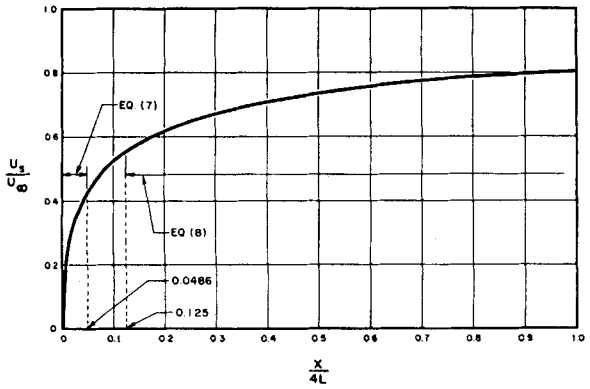

Fig. 4. Surface velocity after Goldstein (*7*, *8*).

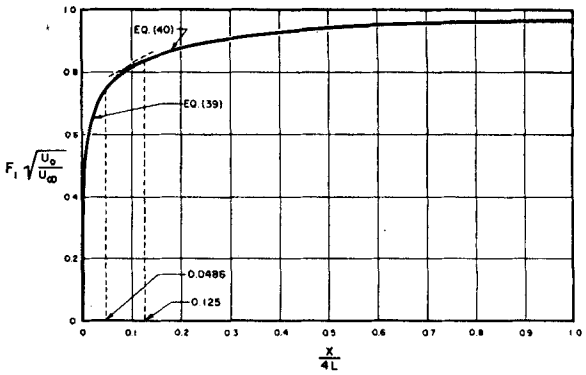

Fig. 5. Effect of nozzle drag on local absorption rate.

Bernoulli equation, the solution of which is

$$f(X) = \frac{U_s(X)}{\sqrt{B + 4\mathfrak{D}\int U_s(X)\,dX}} \tag{27}$$

Hence for any given surface velocity the reduced coordinate η is given by

$$\eta = \frac{YU_s(X)}{\sqrt{B + \mathfrak{D}\int U_s(X)\,dX}} \tag{28}$$

The constant B is evaluated by means of Equation (18*a*), which requires that $\eta(X, Y) \to \infty$ in the limit as $X \to 0$, or else through some other boundary condition in X.

Local absorption rate, rather than the concentration distribution given by Equation (26), is required for absorption predictions:

$$N = -\mathfrak{D}\left(\frac{\partial C}{\partial Y}\right)_{Y=0} = \frac{2}{\sqrt{\pi}}(C_e - C_0)\,\mathfrak{D}f(X) \tag{29}$$

For an idealized jet throughout which velocity is constant (equal to $U_0 = 4q/\pi D_0^2$) it follows from Equations (27) and (29) that

$$N_* = \frac{1}{\sqrt{\pi}}(C_e - C_0)\sqrt{\frac{\mathfrak{D}U_0}{X}} \tag{30}$$

It is convenient to refer absorption rate to this rate for an ideal jet; the ratio is

$$\frac{N}{N_*} = 2f\sqrt{\frac{\mathfrak{D}X}{U_0}} = \frac{2U_s(X)}{\sqrt{\dfrac{\mathfrak{D}X}{U_0\left[B + 4\mathfrak{D}\int U_s(X)\,dX\right]}}} \tag{31}$$

Finally the total absorption rate of solute gas by a jet of length h is obtained by integration over jet length:

$$\phi = \int_0^h \pi D(X)N(X)\,dX \tag{32}$$

For an ideal jet the diameter as well as velocity is constant; hence

$$\phi_* = 2(C_e - C_0)\,D_0\sqrt{\pi\,\mathfrak{D}U_0h} = 4(C_e - C_0)\sqrt{\mathfrak{D}qh} \tag{33}$$

Approximate Solution for Absorption Rate

An exact prediction of absorption rate requires accurate knowledge of the velocity distribution near the surface of a jet affected simultaneously by viscous drag in the nozzle and by gravitational acceleration. The combined effect is not accurately known; however the separate effects can be assessed from the estimates of surface velocity provided by Equations (7) to (9) and can then be combined to give a fairly accurate prediction of absorption rate. The method of combination can be explained as follows.

On the basis of Equations (7), (8), (9), and (31) the functional dependence of local absorption rate can be written as

$$\frac{N}{N_*} = F(\mathfrak{D}, U_0, U_\infty, 4l, g_L, X) \tag{34}$$

Purely dimensional considerations lead immediately to a more fruitful, functional relationship in terms of dimensionless variables:

$$\frac{N}{N_*} = F\left(\frac{U_0X}{\mathfrak{D}}, \frac{U_\infty}{U_0}, \frac{4l}{X}, \frac{g_LX}{U_0^2}\right) = F(\mathfrak{N}_P, \mathfrak{N}_u, \mathfrak{N}_l, \mathfrak{N}_F) \tag{35}$$

If the first two dimensionless groups are regarded as fixed parameters in the problem, expansion of Equation (35) in a Maclaurin series yields

$$\frac{N}{N_*} = F(0,0) + \mathfrak{N}_l\left(\frac{\partial F}{\partial \mathfrak{N}_l}\right)_{0,0} + \mathfrak{N}_F\left(\frac{\partial F}{\partial \mathfrak{N}_F}\right)_{0,0} + \frac{\mathfrak{N}_l^2}{2}\left(\frac{\partial^2 F}{\partial \mathfrak{N}_l^2}\right)_{0,0} + \mathfrak{N}_l\mathfrak{N}_F\left(\frac{\partial^2 F}{\partial \mathfrak{N}_l\,\partial \mathfrak{N}_F}\right)_{0,0} + \frac{\mathfrak{N}_F^2}{2}\left(\frac{\partial^2 F}{\partial \mathfrak{N}_F^2}\right)_{0,0} \tag{36}$$

Now the local absorption rate must approach that into an ideal jet as viscous drag in the nozzle and gravitational acceleration approach zero; therefore $F(0, 0)$ is unity. After evaluation at $\mathfrak{N}_l = \mathfrak{N}_F = 0$, the various partial derivatives may be replaced by constants, say α_1, β_1, γ_{11}, etc., giving

$$\frac{N}{N_*} = -1 + (1 + \alpha_1\mathfrak{N}_l + \alpha_2\mathfrak{N}_l^2 + \cdots) + (1 + \beta_1\mathfrak{N}_F + \beta_2\mathfrak{N}_F^2 + \cdots) + \gamma_{11}\mathfrak{N}_l\mathfrak{N}_F + \cdots \tag{37}$$

(higher-order interaction terms)

Here the first series may be identified with jet operation in a vanishingly small gravitational field, that is with $F_1 = F(\mathfrak{N}_l, 0)$, and the second series may be identified with operation in the absence of nozzle drag, that is with $F_2 = F(0, \mathfrak{N}_F)$. It then follows (provided certain mathematical conditions are satisfied) that for sufficiently small values of the nozzle drag and Froude numbers the local absorption rate is given to a good approximation by

$$\frac{N}{N_*} = -1 + F_1\left(\frac{4l}{X}\right) + F_2\left(\frac{g_LX}{U_0^2}\right) \tag{38}$$

where first- and higher- order interaction terms have been neglected.

The functions F_1 and F_2 are obtained from the estimates of surface velocity and from Equation (31). From Equation (7)

$$F_1 = \sqrt{\frac{4a_1U_\infty\xi}{3U_0}}\cdot\frac{1 - a_2\xi^3 + a_3\xi^6}{\sqrt{1 - \dfrac{4a_2\xi^3}{7} + \dfrac{2a_3\xi^6}{5}}} \tag{39}$$

$$\xi = \left(\frac{X}{4l}\right)^{\frac{1}{3}}; \qquad \frac{X}{4l} \leq 0.0486$$

TABLE 2.

X, cm.	$\mathfrak{N}_l$	F_1, Equation (39) or (40)	$\mathfrak{N}_F$	F_2, Equation (42)	N/N_*, Equation (38)	D/D_0	ϕ/ϕ_*	h, cm.
$D_0 = 0.1535$ cm., $U_0 = 271$ cm./sec., $4l = 0.352$ cm., $U_\infty = 292$ cm./sec.								
0.01	35.2	0.720	0.00013	1.000	0.720	1.000	0.545	0.01
0.1	3.52	0.937	0.00133	1.001	0.938	0.982	0.786	0.1
1	0.352	1.026	0.0133	1.010	1.036	0.968	0.916	1
10	0.0352	1.038	0.133	1.091	1.129	0.924	0.988	10
$D_0 = 0.1535$ cm., $U_0 = 145$ cm./sec., $4l = 0.172$ cm., $U_\infty = 150$ cm./sec.								
0.005	34.4	0.710	0.00047	1.000	0.710	1.000	0.545	0.005
0.05	3.44	0.923	0.00467	1.001	0.924	0.987	0.762	0.05
0.5	0.344	1.009	0.0467	1.017	1.026	0.966	0.911	0.5
5	0.0344	1.019	0.467	1.149	1.168	0.889	0.993	5

where the constant B of Equation (31) has been taken as zero in accordance with Equation (18a). From Equation (8)

$$F_1 = \sqrt{\frac{U_\infty}{U_0}} \frac{1 - \frac{a_4}{\sqrt{x}} - \frac{a_5}{x}}{\sqrt{1 - \left(\frac{4l}{X}\right)(2a_4\sqrt{x} + a_5 \ln x - 0.0956)}} \qquad (40)$$

$$x = \frac{X}{4l} + 0.13; \qquad \frac{X}{4l} \geq 0.125$$

where B has been set equal to 0.0956 ($16l\,\mathfrak{D}U_\infty$) to give a smooth transition from Equation (39) in the region $0.0486 < X/4l < 0.125$ (Figure 5). From Equation (9)

$$F_2 = \sqrt{\left(\frac{3g_L X}{U_0^2}\right) \frac{[1 + (2g_L X/U_0^2)]}{[1 + (2g_L X/U_0^2)]^{\frac{3}{2}} - 1}} \qquad (41)$$

$$= \sqrt{\frac{1 + (2g_L X/U_0^2)}{1 + \frac{(2g_L X/U_0^2)}{4} - \frac{(2g_L X/U_0^2)^2}{24} + \cdots}} \qquad (42)$$

The calculation of the parameters l and U_0 has already been described. The core velocity within the emerging jet was evaluated from the average velocity, the assumed form of the velocity distribution in the boundary layer, and the inferred boundary-layer thickness at the nozzle by means of

$$U_\infty = \frac{U_0}{1 - \frac{3b}{4} - \frac{b^2}{5}} \qquad (43)$$

Comparison with Experimental Results

By the use of the foregoing equations absorption rates at 25°C. of carbon dioxide into several laminar water jets were predicted. The diffusivity of carbon dioxide in water at 25°C. was taken as 1.97×10^{-5} sq. cm./sec., and the solubility at the same temperature and 760 mm. Hg partial pressure was taken as 3.39×10^{-5} g.-mole/cc. The initial concentration, was assumed to be zero, the water having been carefully stripped of dissolved gas before use (*16*).

The order of magnitude of the adjustments to the reference local-absorption rate is indicated in Table 2, in which representative values are listed for jets produced with a 1.535-mm. I.D. brass nozzle at flow rates of 5 and 2.6 cc./sec. Equation (32) with Equation (38) was integrated numerically to arrive at the predicted total absorption rates plotted as full curves in Figure 6. The predicted absorption rates for an ideal jet, according to Equation (33), are plotted for comparison as broken lines.

Experimentally determined absorption rates for nominal contact times ranging from 0.003 to 0.04 sec. are also plotted in Figure 6. Details of the experimental procedure have been reported elsewhere (*16*, *17*). In brief, feed and effluent water samples were drawn with the apparatus operating at steady state. Due precaution was taken to prevent transfer of carbon dioxide to or from the samples. Analysis for dissolved carbon dioxide depended upon the precipitation in basic solution of carbonate ion as barium carbonate, followed by back titration of excess hydroxyl ion with standard acid to the carbonate-bicarbonate end point. Both the precision and accuracy of the analysis were found to be about 0.4 p.p.m.; the range of concentrations analyzed in the effluent water was 10 to 44 p.p.m. That the reproducibility of replicate runs was, with few exceptions, excellent can be seen from the data. The agreement of experimental and predicted absorption rates is very good.

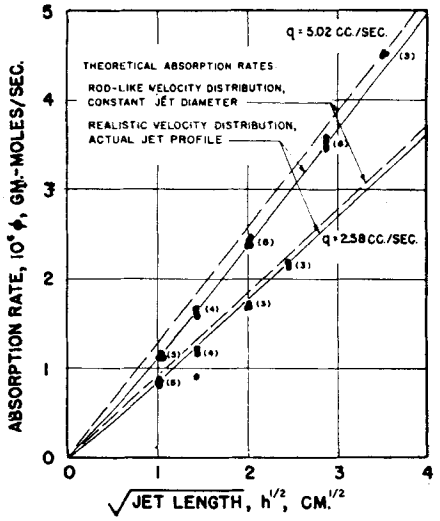

Fig. 6. Carbon dioxide absorption into water.

DISCUSSION

The experimental and predicted absorption rates agree closely, but this fact alone verifies neither the approximate solution of the diffusion equation from which the predictions arise nor the particular set of boundary conditions used to obtain that solution. Before any conclusion is drawn, it is necessary to consider the extent to which the approximate solution may deviate from the exact solution. In over-all absorption rate the former leads to predictions differing from those based on the assumption of an ideal jet by no more than 10%. Such deviation may be regarded as a first perturbation to the ideal-jet absorption rate, caused by the disturbing influences of viscous drag in the nozzle and gravitational acceleration. Now the principal part of the unknown second perturbation is proportional to the product of the already small disturbing influences [Equations (37) and (38)] and may reasonably be expected to be about 1% of the ideal-jet prediction; the higher-order perturbations should be proportionately smaller. It is therefore quite unlikely that the predictions based on the approximate solution are more than 2 or 3% in error, even under the conditions of the lowest absorption rates measured, for which the deviation from ideal-jet behavior was greatest.

Thus the data substantiate the physical model underlying the theoretical predictions; in particular, they confirm the validity of the asumption of thermodynamic equilibrium between gaseous and liquid phases everywhere on the jet surface [Equation (19)]. This matter has been discussed in detail by the authors in an earlier paper (*17*).

ACKNOWLEDGMENT

Thanks are due M. M. Wendel and Stanley Corrsin for helpful discussions of portions of this work and W. J. Baur for

assistance with some of the measurements. The investigation was made possible in part by National Science Foundation and Shell Fellowship Committee fellowships received by L. E. Scriven.

APPENDIX

The nature of the problem of absorption into an accelerating liquid flow is illustrated by a simple example. For a two-dimensional flow directed toward a sink at the origin and bounded by free streamlines at the acute angles $\pm\ \theta_0$ in polar coordinates the potential and stream functions are, respectively,

$$\Phi = R_0 U_0 \ln R$$

$$\Psi = R_0 U_0 \theta$$

where U_0 is the radial velocity at distance R_0 from the origin. Such a flow corresponds to a two-dimensional liquid jet in a certain body force field. If one considers absorption along the free streamlines between R_0 and R, $0 \ll R < R_0$, the appropriate diffusion problem is

$$U\frac{\partial C}{\partial R} = \mathfrak{D}\left(\frac{\partial^2 C}{\partial R^2} + \frac{1}{R}\frac{\partial C}{\partial R} + \frac{1}{R^2}\frac{\partial^2 C}{\partial \theta^2}\right)$$

$$C(R_0\ ,\ \theta) = C_0$$

$$C(R,\ \pm\ \theta_0) = C_e$$

$$\frac{\partial C}{\partial R}(R,\ 0) = 0$$

where the radial velocity is related to the potential function by

$$U = \frac{\partial \Phi}{\partial R}$$

With the usual transformation for diffusion in potential flow, in which the potential and stream functions are taken as the independent variables, and with diffusion along the stream tubes neglected, there follows

$$\frac{\partial C}{\partial \Phi} = \mathfrak{D}\frac{\partial^2 C}{\partial \Psi^2}$$

$$C(\Phi_0\ ,\ \Psi) = C_0\ ,\qquad \Phi_0 = R_0 U_0 \ln R_0$$

$$C(\Phi,\ \pm\ \Psi_0) = C_e\ ,\qquad \Psi_0 = R_0 U_0 \theta_0$$

$$\frac{\partial C}{\partial \Psi}(\Phi,\ 0) = 0$$

which is virtually identical to the problem of diffusion into an infinite sheet, the solution of which is well known. For small values of $\Phi_0 - \Phi$ (short exposure times) the local rate of absorption is expressed conveniently as

$$N = (C_e - C_0)\cdot\sqrt{\frac{\mathfrak{D}U_0}{\pi R_0 (R/R_0)^2 \ln (R_0/R)}}\cdot\left\{1 + 2\sum_{n=1}^{\infty}(-1)^n \cdot \exp\left[\frac{n^2 R_0 U_0 {\theta_0}^2}{\mathfrak{D}\ln (R/R_0)}\right]\right\}$$

If the distance $R_0 - R$ is sufficiently short, the penetration depth of absorbed material is small compared with the width of the flow and only the first term within the braces need be retained. Then the local absorption rate is given by

$$N = (C_e - C_0)\cdot\sqrt{\frac{\mathfrak{D}U_0}{\pi R_0 (1-x)^2 \ln [1/(1-x)]}}$$

where now $x = (R_0 - R)/R_0$.

This problem can also be solved by the method presented herein. Instead of the polar coordinates just used, rectangular coordinates with the origin in the free streamline at R_0 are employed. With this transformation the surface velocity is

$$U_s = \frac{R_0 U_0}{R_0 - X}$$

and the velocity normal to the free streamline is

$$V = -\frac{R_0 U_0 Y}{(R_0 - X)^2 + Y^2}$$

For shallow penetration depths Y is small in the region of interest, and V is given to a good approximation by

$$V \cong -\frac{R_0 U_0 Y}{(R_0 - X)^2}$$

which can also be obtained with the use of Equation (14). From Equations (27) and (29) for local absorption rate, given the surface velocity, the result is again found to be

$$N = (C_e - C_0)\cdot\sqrt{\frac{\mathfrak{D}U_0}{\pi R_0 (1-x)^2 \ln [1/(1-x)]}}$$

There is of course no flow across the streamlines (lines of constant Ψ), but for $Y > 0$ there is a velocity component in the direction normal to the interface which must be accounted for when the diffusion equation is written in rectangular coordinates with the origin in the interface.

NOTATION

a = dimensionless constants, Equations (7) and (8)
b = δ/R_0, dimensionless boundary-layer thickness
B = constant in Equation (27), cm.⁴/sec.²
C = concentration, g.-moles/cc.
C_0 = initial concentration
D = jet diameter, cm.
$\mathfrak{D}$ = diffusion coefficient, sq. cm./sec.
f = function defined by Equation (27)
g_L = local acceleration of gravity, cm./sec.²
h = jet length, cm.
l = equivalent length of flat plate, cm.
N = local absorption rate, g.-moles/(sq. cm.)(sec.)
$\mathfrak{N}_F$ = $g_L X/U_0^2$, Froude number
$\mathfrak{N}_P$ = $U_0 X/\mathfrak{D}$, Peclet number
$\mathfrak{N}_u$ = U_∞/U_0, velocity ratio
$\mathfrak{N}_l$ = $4l/X$, nozzle-drag number
q = volumetric flow rate, cc./sec.
R = jet radius, cm.
U = axial component of velocity, cm./sec.
V = radial component of velocity, cm./sec.
x = $(X/4l) + 0.13$, dimensionless variable, Equation (8)
X = axial coordinate, cm.
Y = radial coordinate, cm.

Greek Letters

δ = boundary-layer thickness, cm.
η = dimensionless variable, Equation (20)
ν = kinematic viscosity, sq. cm./sec.
ξ = $(X/4l)^{1/3}$, dimensionless variable, Equation (7)
ϕ = total absorption rate, g.-moles/sec.

Subscripts

e = equilibrium
0 = nozzle exit
s = surface
∞ = core
$*$ = ideal jet

LITERATURE CITED

1. Birkhoff, Garrett, "Hydrodynamics," Princeton Univ. Press, Princeton, N. J. (1950).
2. Cullen, E. J., and J. F. Davidson, *Trans. Faraday Soc.*, **53**, 113 (1957).
3. Danckwerts, P. V., and A. M. Kennedy, *Trans. Inst. Chem. Engrs. (London)*, **32**, S49 (1954).
4. Dirken, M. N. J., and H. W. Mook, *Biochem. Z.*, **219**, 452 (1930).
5. Edwards, G., R. Robertson, F. Rumford, and J. Thomson, *Trans. Inst. Chem. Engrs. (London)*, **32**, S6 (1954).
6. Eipper, J. E., thesis, Univ. Delaware, Newark (1955).
7. Goldstein, Sydney, *Proc. Cambridge Phil. Soc.*, **26**, 1 (1930).
8. ———, *Proc. Roy. Soc. (London)*, **A142**, 545 (1933).
9. Hammerton, D., and F. H. Garner, *Trans. Inst. Chem. Engrs. (London)*, **32**, S18 (1954).
10. Hughes, R. R., and E. R. Gilliland, *Chem. Eng. Progr. Symposium Ser.* No. 16, **51**, 101 (1955).
11. Lynn, Scott, J. R. Straatemeier, and H. Kramers, *Chem. Eng. Sci.*, **4**, 49, 58 (1955).
12. Manogue, W. H., Ph.D. dissertation, Univ. Delaware, Newark (1957).
13. Matsuyama, Takuzo, *Mem. Fac. Eng. Kyoto Univ.*, **15**, No. 11, 142 (1953) (in English).
14. Rideal, E. K., and K. L. Sutherland, *Trans. Faraday Soc.*, **48**, 1109 (1952).
15. Schlichting, Hermann, "Boundary Layer Theory," McGraw-Hill, New York (1955).
16. Scriven, L. E., Ph.D. dissertation, Univ. Delaware, Newark (1956).
17. ———, and R. L. Pigford, *A.I.Ch.E. Journal*, **4**, 439 (1958).
18. Vielstich, Wolf, *Chem.-Ing.-Tech.*, **28**, 543 (1956).
19. Vivian, J. E., and D. W. Peaceman, *A.I.Ch.E. Journal*, **2**, 437 (1956).

Manuscript received July 22, 1958; revision received January 20, 1959; paper accepted January 22, 1959.